

Received April 24, 2020, accepted May 7, 2020, date of publication May 11, 2020, date of current version May 22, 2020.

Digital Object Identifier 10.1109/ACCESS.2020.2994004

Stabilization of Robots With a Regulator Containing the Sigmoid Mapping

DANY IVAN MARTINEZ¹, JOSÉ DE JESÚS RUBIO¹, (Member, IEEE), TOMAS MIGUEL VARGAS¹, VICTOR GARCIA¹, GENARO OCHOA¹, RICARDO BALCAZAR¹, DAVID RICARDO CRUZ¹, ARTURO AGUILAR¹, JUAN FRANCISCO NOVOA¹, AND CARLOS AGUILAR-IBAÑEZ²

¹Sección de Estudios de Posgrado e Investigación, Esime Azcapotzalco, Instituto Politécnico Nacional, México City 02250, México

²Centro de Investigación en Computación, Instituto Politécnico Nacional, México City 07738, México

Corresponding author: José de Jesús Rubio (rubio.josedejesus@gmail.com)

This work was supported in part by the Instituto Politécnico Nacional, in part by the Consejo Nacional de Ciencia y Tecnología, in part by the Secretaría de Investigación y Posgrado, and in part by the Comisión de Operación y Fomento de Actividades Académicas.

ABSTRACT Actuators nonlinearities are unknown external perturbations in robots, which are unwanted because they can severely limit their performance. This research is focused on the stabilization of robots subject to actuators nonlinearities with a regulator containing the sigmoid mapping. Our regulator has the following three main characteristics: a) a sigmoid mapping is used to ensure boundedness of the regulator law terms, b) the chattering is reduced by the usage of the saturation mapping instead of the signum mapping, and c) the stabilization is ensured by the Lyapunov analysis. Finally, we evaluate our regulator for the stabilization of two robots.

INDEX TERMS Stabilization, regulator, sigmoid, mapping, robot.

I. INTRODUCTION

The nonlinear uncertainties and external perturbations are unwanted characteristics in nonlinear models because they can severely limit their performance or damage their components; this fact has been drawing much interest in the community for a long time [1]–[4]. The linear quadratic regulator is one approach used to reach constant paths in linear models, it is called optimization [5]–[8]. Different to the mentioned research, a regulator is one approach used to reach constant paths in nonlinear models subject to nonlinear uncertainties or external perturbations, it is called stabilization [2], [3].

There is some research of regulators focused on the stabilization of nonlinear models subject to nonlinear uncertainties or external perturbations. Authors addressed regulators for stabilization of microgrids in [9], [10], and [11]. In [12]–[14], and [15], authors focused fuzzy sliding mode regulators of robotic exoskeletons and robotic manipulators. Authors employed neural network sliding mode regulators of wheeled aerial vehicles and robotic manipulators in [16]–[18], and [19]. In [20]–[22], and [23], authors detailed sliding mode regulators based on observers

The associate editor coordinating the review of this manuscript and approving it for publication was Qiu ye Sun¹.

of robotic exoskeletons and quadrotors. Authors analyze proportional derivative sliding model regulators of overhead cranes and inverted pendulums in [24]–[26], and [27]. In [28]–[30], and [31], authors addressed robust sliding model regulators of parallel manipulators and quadrotors. Authors discussed regulators for stabilization of multiple converters in [32], [33], and [34].

The aforementioned research is divided in two big groups where [16]–[19], [21], [22], [24]–[26], [29], [32]–[34] are focused on the stabilization of nonlinear models subject to nonlinear uncertainties, and [9]–[15], [20], [23], [27], [28], [30], [31] are focused on the stabilization of nonlinear models subject to external perturbations. It is important to note that in most of the cases the nonlinear uncertainties or external perturbations are unknown. Hence, the stabilization of nonlinear models where the nonlinear uncertainties or external perturbations are unknown is of great interest.

Actuators nonlinearities are a kind of external perturbations in the robots nonlinear models yielded by the interaction of actuators with the environment [1]–[4]. This research is focused on the stabilization of robots subject to actuators nonlinearities with a regulator containing the sigmoid mapping. Our regulator has the following three main characteristics: a) we utilize the sliding mode in our regulator to compensate the actuators nonlinearities and gravity terms, b) we also use

the proportional derivative approach in our regulator to reach the stabilization of the robots positions; and c) we ensure the stabilization of the regulator error by the Lyapunov analysis.

There are other two issues in a regulator that could limit its performance: a) when boundedness of the regulator law terms is not ensured, and b) when chattering of the signum mapping is increased. The mentioned issues are solved in our regulator as following: a) taking into account that the sigmoid mapping is used in a neural network to ensure its boundedness [16]–[19], we use the sigmoid mapping to ensure boundedness of the regulator law terms, b) taking into account that the saturation mapping is used to reduce its chattering without ensuring its stabilization [28]–[31], we reduce the chattering by the usage of the saturation mapping while we ensure the stabilization.

This research is structured as following. In section II, we present the nonlinear model of robots, and the proportional derivative and sliding mode regulators. In section III, we present a regulator containing the sigmoid mapping for the stabilization of robots. In section IV, we evaluate our regulator for the stabilization of two robots. In section V, we express the conclusions and future research.

II. SOME PROPERTIES OF ROBOTS

In this section we describe some properties of robots such as their nonlinear model, and the proportional derivative and sliding mode regulators.

We define the nonlinear model for the robots with n degrees of freedom in the joint space as [1], [2], [4]:

$$Q(p)\ddot{p} + C(p, \dot{p})\dot{p} + O(p) = \tau, \quad (1)$$

$p \in \mathfrak{R}^{n \times 1}$ as the position, $\dot{p} \in \mathfrak{R}^{n \times 1}$ as the speed in the robot, $Q(p) \in \mathfrak{R}^{n \times n}$ as the robot inertia matrix which is symmetric and positive definite, $C(p, \dot{p}) \in \mathfrak{R}^{n \times n}$ as the centripetal and Coriolis terms, and $O(p)$ as the gravity terms, τ as the actuators nonlinearities.

We express the states and actuators nonlinearities as:

$$\begin{aligned} w_1 &= p \in \mathfrak{R}^{n \times 1}, \\ w_2 &= \dot{p} \in \mathfrak{R}^{n \times 1}, \\ e &= \tau \in \mathfrak{R}^{n \times 1}, \end{aligned} \quad (2)$$

$w_1 = [w_{11} \ w_{12}]^T = [p_1 \ p_2]^T$, $w_2 = [w_{21} \ w_{22}]^T = [\dot{p}_1 \ \dot{p}_2]^T$. Then, we rewrite the nonlinear model of the equation (1) as:

$$\begin{aligned} \dot{w}_1 &= w_2, \\ Q(w_1)\dot{w}_2 + C(w_1, w_2)w_2 + O(w_1) &= e, \end{aligned} \quad (3)$$

$Q(w_1)$, $C(w_1, w_2)$, $O(w_1)$ as in (1).

We represent the actuators nonlinearities e as [1]–[4]:

$$e = \begin{cases} n_r (v - w_r) & v \geq w_r \\ 0 & w_l < v < w_r \\ n_l (v - w_l) & v \leq w_l, \end{cases} \quad (4)$$

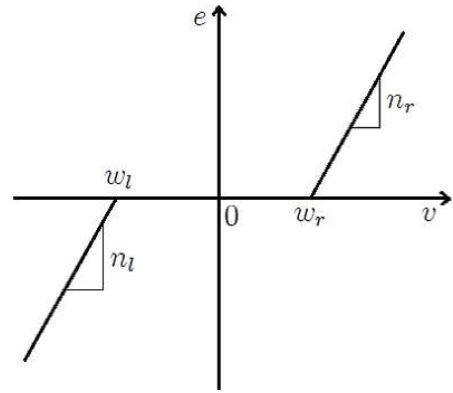


FIGURE 1. The actuator nonlinearities.

n_r , n_l , w_r and w_l as constant terms for the actuators nonlinearities. Note that v is the input of the actuators nonlinearities. We show the actuators nonlinearities in Figure 1.

The actuators nonlinearities of robots are symmetric as $n_r = n_l$ in (4); consequently, we can express the actuators nonlinearities e of (4) as:

$$\begin{aligned} e &= \begin{cases} n_l (v - w_r) & v \geq w_r \\ 0 & w_l < v < w_r \\ n_l (v - w_l) & v \leq w_l, \end{cases} \\ \Rightarrow e &= \begin{cases} n_l v & v \geq w_r \\ n_l v & w_l < v < w_r \\ n_l v & v \leq w_l \end{cases} + \begin{cases} -n_l w_r & v \geq w_r \\ -n_l v & w_l < v < w_r \\ -n_l w_l & v \leq w_l, \end{cases} \end{aligned} \quad (5)$$

after some arranges the actuators nonlinearities e of (5) are expressed as:

$$\begin{aligned} e &= n_l v - h(v), \\ h(v) &= \begin{cases} n_l w_r & v \geq w_r \\ n_l v & w_l < v < w_r \\ n_l w_l & v \leq w_l, \end{cases} \end{aligned} \quad (6)$$

with $h(v)$ as the nonlinearities. We note that the nonlinearities $h(v)$ are bounded as:

$$|h(v)| \leq \bar{h}, \quad (7)$$

We will use the next property in a posterior section to reach the stabilization of our regulator.

Property 1: We express the centripetal and Coriolis matrix as skew-symmetric and this matrix complies the relationship:

$$w^T \left(\dot{Q}(w_1) - 2C(w_1, w_2) \right) w = 0, \quad (8)$$

$w = [w_1, w_2]^T$, $Q(w_1)$, and $C(w_1, w_2)$ as in (3).

Now, we express the proportional derivative and sliding mode regulators because they will be used for the results in a posterior section.

We detail a proportional derivative regulator as [24], [25]:

$$v = \frac{1}{n_l} (-K_p \tilde{w}_1 - K_d \tilde{w}_2), \quad (9)$$

$\tilde{w}_1 = w_1 - w_1^d \in \mathbb{R}^{n \times 1}$, $\tilde{w}_1 \in \mathbb{R}^{n \times 1}$ as the position regulator error, $w_1 \in \mathbb{R}^{n \times 1}$ as the position, $w_1^d \in \mathbb{R}^{n \times 1}$ as the constant desired position, $\tilde{w}_2 = w_2 \in \mathbb{R}^{n \times 1}$ as the speed regulator error, $K_p, K_d \in \mathbb{R}^{n \times n}$ as positive definite, symmetric and constant matrices, $w_1^d \in \mathbb{R}^{n \times 1}$ as the desired reference, n_l as a actuators nonlinearities term.

We detail a sliding mode regulator as [2], [3]:

$$v = \frac{1}{n_l} (-K_p \tilde{w}_1 - K_d \tilde{w}_2 - K \text{sign}(\tilde{w}_2)),$$

$$\text{sign}(\tilde{w}_2) = \begin{cases} 1 & \tilde{w}_2 > 0 \\ 0 & \tilde{w}_2 = 0 \\ -1 & \tilde{w}_2 < 0, \end{cases} \quad (10)$$

$\tilde{w}_1 = w_1 - w_1^d \in \mathbb{R}^{n \times 1}$, $\tilde{w}_1 \in \mathbb{R}^{n \times 1}$ as the position regulator error, $w_1 \in \mathbb{R}^{n \times 1}$ as the position, $w_1^d \in \mathbb{R}^{n \times 1}$ as the constant desired position, $\tilde{w}_2 = w_2 \in \mathbb{R}^{n \times 1}$ as the speed regulator error, $K_p, K_d \in \mathbb{R}^{n \times n}$ as positive definite, symmetric and constant matrices, $w_1^d \in \mathbb{R}^{n \times 1}$ as the desired reference, $\text{sign}(\cdot)$ as the signum mapping, n_l as a actuators nonlinearities term.

Remark 1: The actuators nonlinearities e of (4) are expressed as the external perturbations of (6) where the nonlinearities $h(v)$ are the external perturbations yielded by the interaction of actuators with the environment.

III. A REGULATOR CONTAINING THE SIGMOID MAPPING

We represent the gravity terms $O(w_1)$ of (3) bounded as:

$$|O(w_1)| \leq \bar{O}, \quad (11)$$

We take into account the stabilization case in this research due to we use the desired speed states as $w_2^d = 0$, and the desired references as constant. We detail a regulator containing the sigmoid mapping v as:

$$v = \frac{1}{n_l} \left(- \left(1 - b(\tilde{w}_1)^2 \right)^T K_p b(\tilde{w}_1) - K_d \tilde{w}_2 - K \text{sat}(\tilde{w}_2) \right),$$

$$\text{sat}(\tilde{w}_2) = \begin{cases} 1 & \tilde{w}_2 > 1 \\ \tilde{w}_2 & |\tilde{w}_2| \leq 1 \\ -1 & \tilde{w}_2 < -1, \end{cases}$$

$$b(\tilde{w}_1) = \frac{1 - \exp(-2\tilde{w}_1)}{1 + \exp(-2\tilde{w}_1)}, \quad (12)$$

$\tilde{w}_1 = w_1 - w_1^d \in \mathbb{R}^{n \times 1}$, $\tilde{w}_1 \in \mathbb{R}^{n \times 1}$ as the position regulator error, $w_1 \in \mathbb{R}^{n \times 1}$ as the position, $w_1^d \in \mathbb{R}^{n \times 1}$ as the constant desired position, $\tilde{w}_2 = w_2 \in \mathbb{R}^{n \times 1}$ as the speed regulator error, $K_p, K_d \in \mathbb{R}^{n \times n}$ as positive definite, symmetric and constant matrices, $\text{sat}(\cdot)$ as the saturation mapping, $b(\cdot)$ as the sigmoid mapping, K as a constant such as $\bar{O} + \bar{h} \leq K$, \bar{O} as in (11), \bar{h} as in (7), n_l as a actuators nonlinearities term. It is important to note that we do not know the behavior of $O(w_1)$, $h(v)$ and we utilize their upper bounds \bar{O} , \bar{h} .

Remark 2: Since w_2 will reach to w_2^d and $w_2^d = 0$, it yields $\tilde{w}_2 = w_2 \cong 0$; consequently, \tilde{w}_2 is bounded, and since $b(\tilde{w}_1)$ and $\text{sat}(\tilde{w}_2)$ also are bounded, it yields that the regulator law terms v for a regulator containing the sigmoid mapping (12) are bounded.

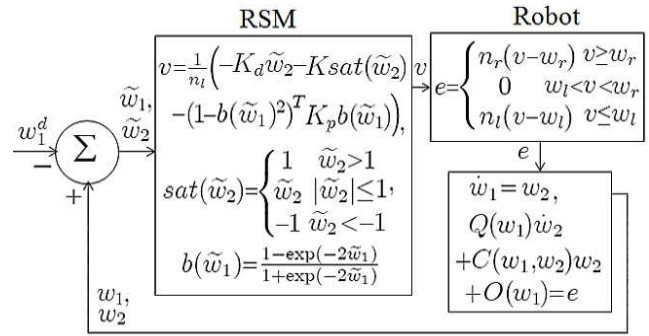


FIGURE 2. A regulator containing the sigmoid mapping.

In Figure 2 we show a regulator containing the sigmoid mapping called RSM for the stabilization of robots called Robot.

Now, we will detail the stabilization of the regulator error.

Theorem 1: The stabilization of the regulator error in the close-loop model of a regulator containing the sigmoid mapping (12) and robots (3) is ensured, and the speed regulator error \tilde{w}_2 will complies with:

$$\limsup_{T \rightarrow \infty} \|\tilde{w}_2\|^2 = 0, \quad (13)$$

T as the final time, $\tilde{w}_2 = w_2$, $|O(w_1)| \leq \bar{O}$, $|h(v)| \leq \bar{h}$, and $\bar{O} + \bar{h} \leq K$.

Proof: We represent the Lyapunov candidate as:

$$L_1 = \frac{1}{2} \tilde{w}_2^T Q(w_1) \tilde{w}_2 + \frac{1}{2} b(\tilde{w}_1)^T K_p b(\tilde{w}_1), \quad (14)$$

$Q(w_1)$ as the positive definite matrix of (3) and K_p as the positive definite matrix of (12). We take into account $\tilde{w}_2 = w_2$ and we substitute (12) into (3), we obtain the closed-loop model as:

$$\begin{aligned} & Q(w_1) \dot{\tilde{w}}_2 + C(w_1, w_2) w_2 + O(w_1) \\ &= e = n_l v - h(v) \\ &= n_l \frac{1}{n_l} \left(- \left(1 - b(\tilde{w}_1)^2 \right)^T K_p b(\tilde{w}_1) - K_d \tilde{w}_2 - K \text{sat}(\tilde{w}_2) \right) - h(v), \\ \implies & Q(w_1) \dot{\tilde{w}}_2 \\ &= - \left(1 - b(\tilde{w}_1)^2 \right)^T K_p b(\tilde{w}_1) \\ &\quad - K_d \tilde{w}_2 - O(w_1) - h(v) - K \text{sat}(\tilde{w}_2) \\ &\quad - C(w_1, w_2) \tilde{w}_2, \end{aligned} \quad (15)$$

We use the fact $\tilde{w}_2 = w_2$, we express the derivative of (14) as:

$$\begin{aligned} \dot{L}_1 &= \tilde{w}_2^T Q(w_1) \dot{\tilde{w}}_2 + \frac{1}{2} \dot{\tilde{w}}_2^T Q(w_1) \tilde{w}_2 \\ &\quad + \tilde{w}_2^T \left(1 - b(\tilde{w}_1)^2 \right)^T K_p b(\tilde{w}_1), \end{aligned} \quad (16)$$

$\dot{\tilde{w}}_1 = \dot{w}_1 - \dot{w}_1^d = w_2 - w_2^d = w_2 = \tilde{w}_2$ and $\dot{\tilde{w}}_2 = \dot{w}_2$. We substitute the last equation of (15) into (16) as:

$$\begin{aligned} \dot{L}_1 &= \tilde{w}_2^T \left(- \left(1 - b(\tilde{w}_1)^2 \right)^T K_p b(\tilde{w}_1) - K_d \tilde{w}_2 \right. \\ &\quad \left. - O(w_1) - h(v) - Ksat(\tilde{w}_2) - C(w_1, w_2) \tilde{w}_2 \right) \\ &\quad + \frac{1}{2} \tilde{w}_2^T \dot{Q}(w_1) \tilde{w}_2 + \tilde{w}_2^T \left(1 - b(\tilde{w}_1)^2 \right)^T K_p b(\tilde{w}_1), \\ \Rightarrow \dot{L}_1 &= -\tilde{w}_2^T K_d \tilde{w}_2 - \tilde{w}_2^T O(w_1) \\ &\quad - \tilde{w}_2^T h(v) - \tilde{w}_2^T Ksat(\tilde{w}_2) \\ &\quad + \frac{1}{2} \tilde{w}_2^T \dot{Q}(w_1) \tilde{w}_2 - \tilde{w}_2^T C(w_1, w_2) \tilde{w}_2 \\ &\quad - \tilde{w}_2^T \left(1 - b(\tilde{w}_1)^2 \right)^T K_p b(\tilde{w}_1) \\ &\quad + \tilde{w}_2^T \left(1 - b(\tilde{w}_1)^2 \right)^T K_p b(\tilde{w}_1), \end{aligned} \quad (17)$$

after some arranges, \dot{L}_1 of (17) is expressed as:

$$\begin{aligned} \dot{L}_1 &= -\tilde{w}_2^T K_d \tilde{w}_2 - \tilde{w}_2^T O(w_1) \\ &\quad - \tilde{w}_2^T h(v) - \tilde{w}_2^T Ksat(\tilde{w}_2) \\ &\quad + \frac{1}{2} \tilde{w}_2^T \left(\dot{Q}(w_1) - 2C(w_1, w_2) \right) \tilde{w}_2, \end{aligned} \quad (18)$$

We use (8) of Property 1 in the equation of (18) as:

$$\dot{L}_1 = -\tilde{w}_2^T K_d \tilde{w}_2 - \tilde{w}_2^T O(w_1) - \tilde{w}_2^T h(v) - \tilde{w}_2^T Ksat(\tilde{w}_2), \quad (19)$$

From (11) $O(w_1) + h(v) \leq |O(w_1)| + |h(v)| \leq \bar{O} + \bar{h} \leq K$,

and from (12) $sat(\tilde{w}_2) = \begin{cases} 1 & \tilde{w}_2 > 1 \\ \tilde{w}_2 & |\tilde{w}_2| \leq 1 \\ -1 & \tilde{w}_2 < -1 \end{cases}$, we represent

the three cases of the saturation mapping. 1) If $\tilde{w}_2 > 1$, then $sat(\tilde{w}_2) = 1$ and $\tilde{w}_2 = |\tilde{w}_2|$, we substitute in (19) as:

$$\begin{aligned} \dot{L}_1 &\leq -\tilde{w}_2^T K_d \tilde{w}_2 + |\tilde{w}_2|^T \bar{O} + |\tilde{w}_2|^T \bar{h} - |\tilde{w}_2|^T K, \\ \Rightarrow \dot{L}_1 &\leq -\tilde{w}_2^T K_d \tilde{w}_2, \end{aligned} \quad (20)$$

2) If $|\tilde{w}_2| \leq 1$, then $sat(\tilde{w}_2) = \tilde{w}_2$ and $\tilde{w}_2^T \tilde{w}_2 = |\tilde{w}_2|^T |\tilde{w}_2|$, we substitute in (19) as:

$$\begin{aligned} \dot{L}_1 &= -\tilde{w}_2^T K_d \tilde{w}_2 + |\tilde{w}_2|^T \bar{O} + |\tilde{w}_2|^T \bar{h} - \tilde{w}_2^T \tilde{w}_2 K, \\ \Rightarrow \dot{L}_1 &= -\tilde{w}_2^T K_d \tilde{w}_2 + |\tilde{w}_2|^T \bar{O} \\ &\quad + |\tilde{w}_2|^T \bar{h} - |\tilde{w}_2|^T |\tilde{w}_2| K, \\ \Rightarrow \dot{L}_1 &= -\tilde{w}_2^T K_d \tilde{w}_2, \end{aligned} \quad (21)$$

due to in this case $|\tilde{w}_2| \leq 1$. 3) If $\tilde{w}_2 < -1$, then $sat(\tilde{w}_2) = -1$ and $\tilde{w}_2 = -|\tilde{w}_2|$, we substitute in (19) as:

$$\begin{aligned} \dot{L}_1 &= -\tilde{w}_2^T K_d \tilde{w}_2 - \left(-|\tilde{w}_2|^T \right) O(w_1) \\ &\quad - \left(-|\tilde{w}_2|^T \right) h(v) - \left(-|\tilde{w}_2|^T \right) K (-1), \\ \Rightarrow \dot{L}_1 &\leq -\tilde{w}_2^T K_d \tilde{w}_2 + |\tilde{w}_2|^T \bar{O} + |\tilde{w}_2|^T \bar{h} - |\tilde{w}_2|^T K, \end{aligned}$$

$$\Rightarrow \dot{L}_1 \leq -\tilde{w}_2^T K_d \tilde{w}_2, \quad (22)$$

The three cases yield the same inequality, from (20), (21), (22) we express:

$$\dot{L}_1 \leq -\tilde{w}_2^T K_d \tilde{w}_2, \quad (23)$$

From [2], [3], the stabilization of the regulator error is ensured. We integrate (23) from 0 to T as:

$$\begin{aligned} \int_0^T \tilde{w}_2^T K_d \tilde{w}_2 dt &\leq L_{1,0} - L_{1,T} \leq L_{1,0}, \\ \Rightarrow \frac{\lambda_{\min}(K_d)}{T} \int_0^T \|\tilde{w}_2\|^2 dt &\leq \frac{1}{T} \int_0^T \tilde{w}_2^T K_d \tilde{w}_2 dt \leq \frac{1}{T} L_{1,0}, \end{aligned} \quad (24)$$

and applying the lim sup to both sides of the last inequality of (24) is:

$$\limsup_{T \rightarrow \infty} \left(\frac{1}{T} \int_0^T \|\tilde{w}_2\|^2 dt \right) \leq \frac{L_{1,0}}{\lambda_{\min}(K_d)} \left(\limsup_{T \rightarrow \infty} \left(\frac{1}{T} \right) \right) = 0, \quad (25)$$

If $T \rightarrow \infty$, then $\|\tilde{w}_2\|^2 = 0$, and it is (13). \square

Remark 3: Our regulator (12) requires to comply with conditions (11), (7) to be applied for the stabilization of robots (3), (4).

IV. RESULTS

In this section, we evaluate a regulator containing the sigmoid mapping of (12) denoted as RSM, a proportional derivative regulator of (9), [24], [25], and a sliding mode regulator of (10), [2], [3] denoted as SM, for the stabilization of the scara and two link robots. Our goal in the regulators is that the paths of the states in robots must follow the paths of desired constant references as fast as possible. The scara and two link robots are chosen due to they are written as (3) and could be employed in pick and place, screwed, printed circuits boards, packaging and labeling, etc. We mainly use the MATLAB software for the results. We utilize the mean square error (MSE), the root mean square error (RMSE), the mean absolute error (MAE), and the mean absolute percent error (MAPE) for the evaluations as:

$$MSE = \left(\frac{1}{T} \int_0^T \tilde{w}^2 dt \right), \quad (26)$$

$$RMSE = \left(\frac{1}{T} \int_0^T \tilde{w}^2 dt \right)^{\frac{1}{2}}, \quad (27)$$

$$MAE = \left(\frac{1}{T} \int_0^T |\tilde{w}| dt \right), \quad (28)$$

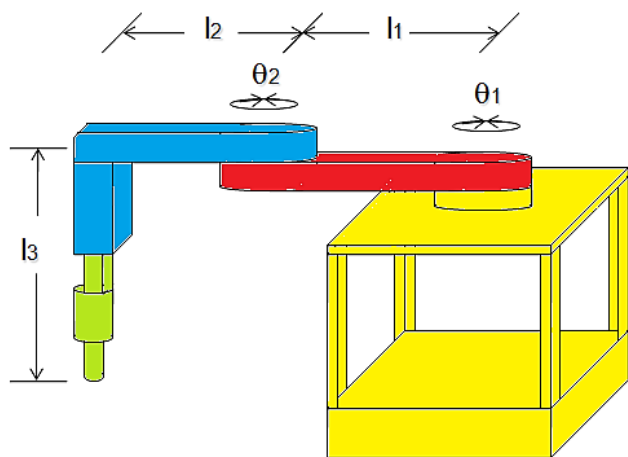


FIGURE 3. Scara robot.

$$MAPE = \left(\frac{100}{T} \int_0^T |\tilde{w}| dt \right), \quad (29)$$

$\tilde{w}^2 = \tilde{w}_{11}^2 + \tilde{w}_{12}^2 + \dots + \tilde{w}_{1n}^2 + \tilde{w}_{21}^2 + \tilde{w}_{22}^2 + \dots + \tilde{w}_{2n}^2$ as the positions and speeds or $\tilde{w}^2 = e_1^2 + e_2^2 + \dots + e_n^2$ as the actuators nonlinearities. $\tilde{w}_{11}^2 = (w_{11} - w_{11}^d)^2$, $\tilde{w}_{12}^2 = (w_{12} - w_{12}^d)^2$, $\tilde{w}_{1n}^2 = (w_{1n} - w_{1n}^d)^2$ as the positions regulators errors, $\tilde{w}_{21}^2 = w_{21}^2$, $\tilde{w}_{22}^2 = w_{22}^2$, $\tilde{w}_{2n}^2 = w_{2n}^2$ as the speeds regulators errors, $e_1^2 = e_1^2$, $e_2^2 = e_2^2$, $e_n^2 = e_n^2$ as the actuators nonlinearities regulators errors, w_{11} , w_{12} , w_{1n} as the positions, w_{21} , w_{22} , w_{2n} as the speeds, and e_1 , e_2 , e_3 as the actuators nonlinearities.

A. SCARA ROBOT

The scara robot has three degrees of freedom, it has two rotary joints and two links configured in horizontal position, it has one linear joint and one link configured in vertical position. We express the scara robot of the Figure 3.

We write the scara robot as (3) and we detail it as:

$$\begin{aligned} \dot{w}_1 &= w_2, \\ Q(w_1)\dot{w}_2 + C(w_1, w_2)w_2 + O(w_1) &= e, \\ Q(w_1) &= \begin{bmatrix} q_{11}(w_1) & q_{12}(w_1) & q_{13}(w_1) \\ q_{21}(w_1) & q_{22}(w_1) & q_{23}(w_1) \\ q_{31}(w_1) & q_{32}(w_1) & q_{33}(w_1) \end{bmatrix}, \\ C(w_1, w_2) &= \begin{bmatrix} c_{11}(w_1, w_2) & c_{12}(w_1, w_2) & c_{13}(w_1, w_2) \\ c_{21}(w_1, w_2) & c_{22}(w_1, w_2) & c_{23}(w_1, w_2) \\ c_{31}(w_1, w_2) & c_{32}(w_1, w_2) & c_{33}(w_1, w_2) \end{bmatrix}, \\ O(w_1) &= [o_1(w_1) \quad o_2(w_1) \quad o_3(w_1)]^T, \end{aligned} \quad (30)$$

and:

$$\begin{aligned} q_{11}(w_1) &= J_{13} + m_2 l_{c1}^2 + m_3 (l_1^2 + l_2^2) \\ &+ m_4 (l_1^2 + l_2^2) + 2l_1 C_2 (m_3 l_{c2} + m_4 l_2), \end{aligned}$$

$$\begin{aligned} q_{12}(w_1) &= q_{21}(w_1) = (m_3 l_{c2}^2 + m_4 l_2^2) + l_1 C_2 (m_3 l_{c2} + m_4 l_2), \\ q_{22}(w_1) &= J_3 + (m_3 l_{c2}^2 + m_4 l_2^2), \\ q_{33}(w_1) &= m_4, \end{aligned} \quad (31)$$

the other terms of $Q(w_1)$ are zero,

$$\begin{aligned} c_{11}(w_1, w_2) &= -2l_1 S_2 (m_3 l_{c2} + m_4 l_2) w_{22}, \\ c_{12}(w_1, w_2) &= -l_1 S_2 (m_3 l_{c2} + m_4 l_2) w_{22}, \\ c_{12}(w_1, w_2) &= 2l_1 S_2 (m_3 l_{c2} + m_4 l_2) w_{21}, \end{aligned} \quad (32)$$

the other terms of $C(w_1, w_2)$ are zero,

$$o_3(w_1) = -m_3 g \quad (33)$$

the other terms of $O(w_1)$ are zero. e as actuators nonlinearities, w_1 as positions, w_2 as speeds, m_2 , m_3 , and m_4 as the masses of the links one, two, and three, $w_{11} = \theta_1$, $w_{12} = \theta_2$, as the angles of the joints one and two in rad, $w_{13} = l_{c3}$ as the length of the link three, in m, g is the acceleration gravity constant. $l_1 = l_2 = 0.3$ m, $l_{c1} = l_1/2$, $l_{c2} = l_2/2$, $m_2 = m_3 = m_4 = 0.3$ kg, $J_{13} = J_1 + J_2 + J_3$, $J_1 = 0.0208$ kgm², $J_2 = J_3 = 0.0127$ kgm², and $g = 9.81$ m/s². $n_r = n_l = 0.5$, $w_r = 0.5$, and $w_l = -0.5$ as the actuators nonlinearities terms.

PD of [24], [25] is expressed by equation (9) with parameters

$$K_p = \begin{bmatrix} 200 & 0 & 0 \\ 0 & 200 & 0 \\ 0 & 0 & 500 \end{bmatrix}, K_d = \begin{bmatrix} 10 & 0 & 0 \\ 0 & 10 & 0 \\ 0 & 0 & 10 \end{bmatrix}.$$

SM of [2], [3] is expressed by equation (10) with parameters

$$K_p = \begin{bmatrix} 200 & 0 & 0 \\ 0 & 200 & 0 \\ 0 & 0 & 500 \end{bmatrix}, K_d = \begin{bmatrix} 10 & 0 & 0 \\ 0 & 10 & 0 \\ 0 & 0 & 10 \end{bmatrix}, K =$$

$$\begin{bmatrix} 1.5 \\ 1.5 \\ 1.5 \end{bmatrix}.$$

RSM of this research is expressed by equation (12)

$$\text{with parameters } K_p = \begin{bmatrix} 200 & 0 & 0 \\ 0 & 200 & 0 \\ 0 & 0 & 500 \end{bmatrix}, K_d =$$

$$\begin{bmatrix} 10 & 0 & 0 \\ 0 & 10 & 0 \\ 0 & 0 & 10 \end{bmatrix}, K = \begin{bmatrix} 1.5 \\ 1.5 \\ 1.5 \end{bmatrix}.$$

We evaluate the actuators nonlinearities in the Figure 4, we evaluate the positions in the Figure 5, we evaluate the speeds in the Figure 6, we show the MSE of (26), the RMSE of (27) in the Table 1, the MAE of (28), and the MAPE of (29) in the Table 2 for the scara robot.

In the Figure 5, since the position and speed of RSM reach better the paths of the constant desired references than the position and speed of PD and SM, we can see that RSM is more efficient than PD and SM. In the Figures 4 and 6, in the RSM the chattering of the actuators nonlinearities and speeds is reduced, while in the SM the chattering of the actuators nonlinearities and speeds is not reduced, and in the PD the actuators nonlinearities and speeds are not stabilized. In the

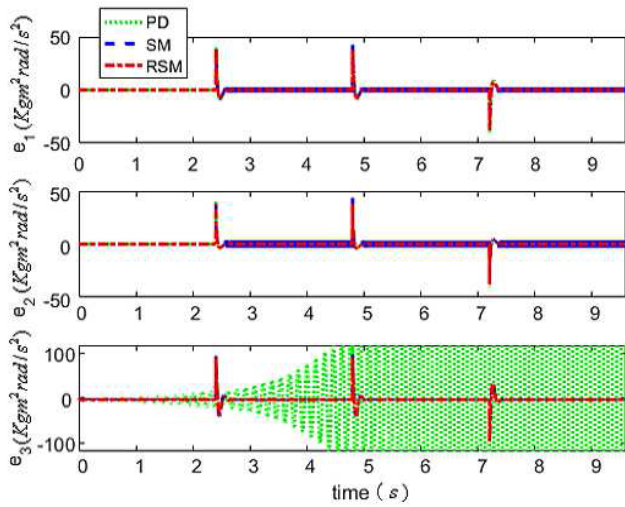


FIGURE 4. Actuators nonlinearities for the scara robot.

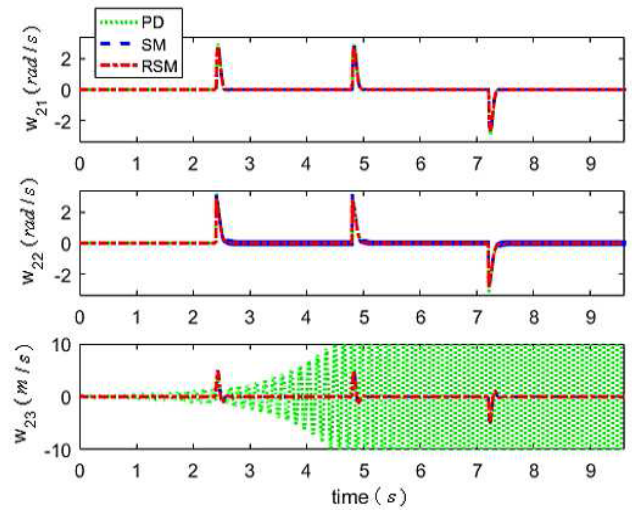


FIGURE 6. Speeds for the scara robot.

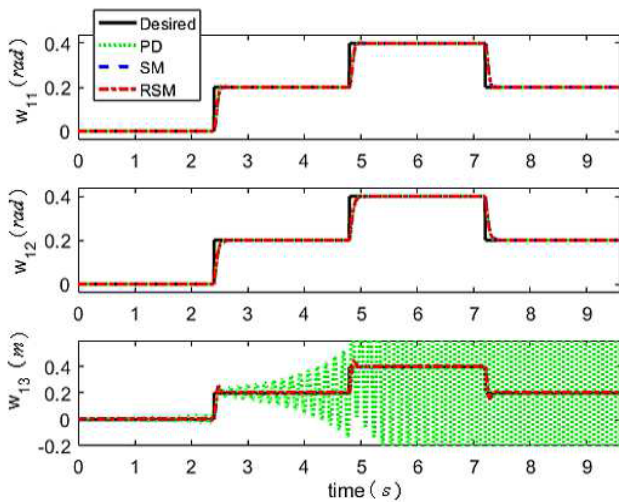


FIGURE 5. Positions for the scara robot.

TABLE 1. MSE and RMSE for the scara robot.

	MSE \tilde{w}	MSE e	RMSE \tilde{w}	RMSE e
PD	39963	5723200	199.9073	2392.3
SM	0.3825	39.7644	0.6184	6.3059
RSM	0.3609	31.0592	0.6008	5.5731

Table 1 and Table 2, since the MSE, RMSE, MAE, and MAPE for the RSM are smaller than for PD and SM, we can show that RSM is more efficient than PD and SM.

B. TWO LINK ROBOT

The two link robot has two degrees of freedom, it has two rotary joints and two links configured in vertical position. We express the two link robot of the Figure 7.

We write the two link robot as (3) and we detail it as:

$$\dot{w}_1 = w_2, \\ Q(w_1)w_2 + C(w_1, w_2)w_2 + O(w_1)$$

TABLE 2. MAE and MAPE for the scara robot.

	MAE \tilde{w}	MAE e	MAPE \tilde{w}	MAPE e
PD	59.5663	698.7547	5956.6	69875
SM	0.5076	4.2425	50.7593	424.2493
RSM	0.4154	2.2464	41.5400	224.6355

$$= e, \\ Q(w_1) = \begin{bmatrix} q_{11}(w_1) & q_{12}(w_1) \\ q_{21}(w_1) & q_{22}(w_1) \end{bmatrix}, \\ C(w_1, w_2) = \begin{bmatrix} c_{11}(w_1, w_2) & c_{12}(w_1, w_2) \\ c_{21}(w_1, w_2) & c_{22}(w_1, w_2) \end{bmatrix}, \\ O(w_1) = [o_1(w_1) \quad o_2(w_1)]^T, \quad (34)$$

and:

$$q_{11}(w_1) = J_{12} + m_2 l_{c2}^2 C_2, \\ q_{22}(w_1) = J_2 + m_2 l_{c2}^2, \quad (35)$$

the other terms of $Q(w_1)$ are zero,

$$c_{12}(w_1, w_2) = -m_2 l_{c2}^2 S_2 w_{21}, \\ c_{21}(w_1, w_2) = m_2 l_{c2}^2 S_2 C_2 w_{21}, \quad (36)$$

the other terms of $C(w_1, w_2)$ are zero,

$$o_2(w_1) = m_2 g l_{c2} C_2, \quad (37)$$

the other terms of $O(w_1)$ are zero. e as actuators nonlinearities, w_1 as positions, w_2 as speeds, m_2 as the mass of the link two in kg, $w_{11} = \theta_1$ and $w_{12} = \theta_2$ as the angles of the joints one and two in rad, g is the acceleration gravity constant, J_1 and J_2 as the inertias in kgm^2 , $C_2 = \cos(w_{12})$, $S_2 = \sin(w_{12})$. $m_2 = 0.34$ kg, $l_2 = 0.293$ m, $l_{c2} = \frac{l_2}{2}$, $J_{12} = J_1 + J_2$, $J_1 = 0.0208$ kgm^2 , $J_2 = 0.0127$ kgm^2 , and $g = 9.81$ m/s^2 . $n_r = n_l = 0.5$, $w_r = 0.5$, and $w_l = -0.5$ as the actuators nonlinearities terms.

PD of [24], [25] is expressed by equation (9) with parameters $K_p = \begin{bmatrix} 500 & 0 \\ 0 & 500 \end{bmatrix}$, $K_d = \begin{bmatrix} 30 & 0 \\ 0 & 30 \end{bmatrix}$.

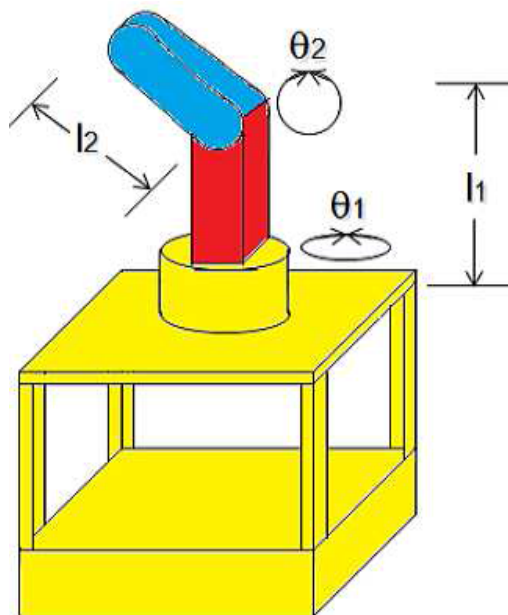


FIGURE 7. Two link robot.

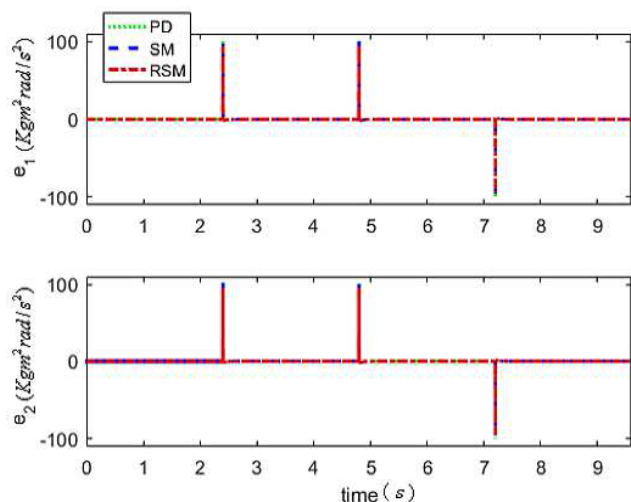


FIGURE 8. Actuators nonlinearities for the two link robot.

SM of [2], [3] is expressed by equation (10) with parameters $K_p = \begin{bmatrix} 500 & 0 \\ 0 & 500 \end{bmatrix}$, $K_d = \begin{bmatrix} 30 & 0 \\ 0 & 30 \end{bmatrix}$, $K = \begin{bmatrix} 1.5 \\ 1.5 \end{bmatrix}$.

RSM of this research is expressed by equation (12) with parameters $K_p = \begin{bmatrix} 500 & 0 \\ 0 & 500 \end{bmatrix}$, $K_d = \begin{bmatrix} 30 & 0 \\ 0 & 30 \end{bmatrix}$, $K = \begin{bmatrix} 1.5 \\ 1.5 \end{bmatrix}$.

We evaluate the actuators nonlinearities in the Figure 8, we evaluate the positions in the Figure 9, we evaluate the speeds in the Figure 10, we show the MSE of (26), the RMSE of (27) in the Table 3, the MAE of (28), and the MAPE of (29) in the Table 4 for the two link robot.

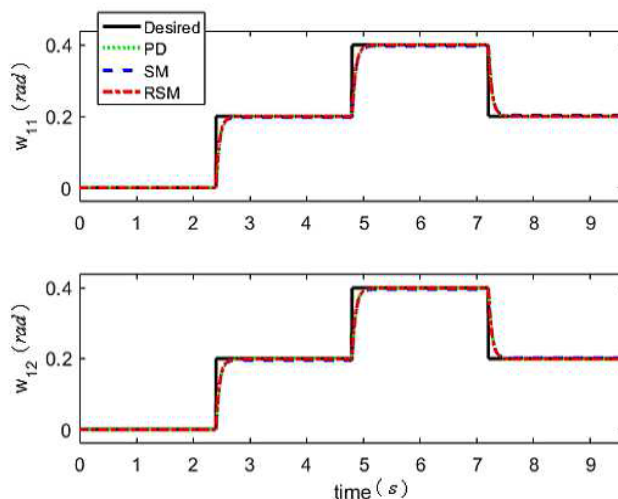


FIGURE 9. Positions for the two link robot.

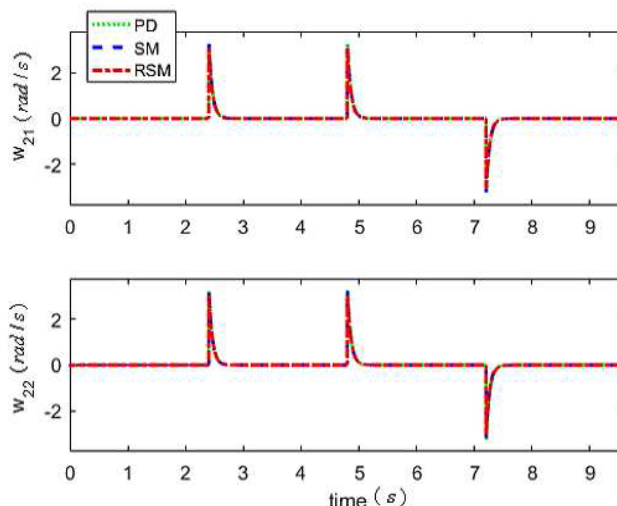


FIGURE 10. Speeds for the two link robot.

TABLE 3. MSE and RMSE for the two link robot.

	MSE \tilde{w}	MSE e	RMSE \tilde{w}	RMSE e
PD	0.1663	3.9605	0.4079	1.9901
SM	0.1628	4.8657	0.4035	2.2058
RSM	0.1606	3.5570	0.4008	1.8860

TABLE 4. MAE and MAPE for the two link robot.

	MAE \tilde{w}	MAE e	MAPE \tilde{w}	MAPE e
PD	0.2611	0.3057	26.1075	30.5730
SM	0.2642	0.5763	26.4210	57.6275
RSM	0.2610	0.3001	26.1008	30.0130

In the Figure 9, since the position and speed of RSM reach better the paths of the constant desired references than the position and speed of PD and SM, we can see that RSM is

more efficient than PD and SM. In the Figures 8 and 10, we can see that in the RSM the chattering of the actuators nonlinearities and speeds is reduced, while in the SM the chattering of the actuators nonlinearities and speeds is not reduced, and in the PD the actuators nonlinearities and speeds are not stabilized. In the Table 3 and Table 4, since the MSE, RMSE, MAE, and MAPE for the RSM are smaller than for PD and SM, we can show that RSM is more efficient than PD and SM.

V. CONCLUSION

In this research, we were focused on the stabilization of robots subject to actuators nonlinearities with a regulator containing the sigmoid mapping. In the results with respect to a proportional derivative regulator and a sliding mode regulator, since the position and speed of our regulator reach better the paths of the constant desired references, and the chattering in our regulator is reduced, we showed that the our regulator is more efficient for the stabilization of two robots. Our regulator illustrates the viability, efficiency, and potential especially important in robots subject to actuators nonlinearities. Our discussed method could also be applied to solve other issues in robots like Coulomb friction, or backlash. As a future research, we will modify our discussed regulator using that some parameters are approximated by the intelligent systems.

ACKNOWLEDGMENT

The authors would like to thank the editors and reviewers for important suggestions and comments to improve this research.

REFERENCES

- [1] G. Peng, C. Yang, W. He, and C. L. P. Chen, "Force sensorless admittance control with neural learning for robots with actuator saturation," *IEEE Trans. Ind. Electron.*, vol. 67, no. 4, pp. 3138–3148, Apr. 2020.
- [2] J. de J. Rubio, "Sliding mode control of robotic arms with deadzone," *IET Control Theory Appl.*, vol. 11, no. 8, pp. 1214–1221, May 2017.
- [3] J. De Jesus Rubio, J. F. Novoa, G. Ochoa, D. Mujica-Vargas, E. Garcia, R. Balcazar, I. Elias, D. R. Cruz, C. F. Juarez, and A. Aguilar, "Structure regulator for the perturbations attenuation in a quadrotor," *IEEE Access*, vol. 7, pp. 138244–138252, 2019.
- [4] F. Wang, Z. Liu, C. L. P. Chen, and Y. Zhang, "Robust adaptive visual tracking control for uncertain robotic systems with unknown dead-zone inputs," *J. Franklin Inst.*, vol. 356, no. 12, pp. 6255–6279, Aug. 2019.
- [5] N. T. K. Son, N. P. Dong, H. V. Long, L. H. Son, and A. Khasan, "Linear quadratic regulator problem governed by granular neutrosophic fractional differential equations," *ISA Trans.*, vol. 97, pp. 296–316, Feb. 2020.
- [6] N. T. K. Son, N. P. Dong, L. H. Son, M. Abdel-Basset, G. Manogaran, and H. V. Long, "On the stabilizability for a class of linear time-invariant systems under uncertainty," *Circuits, Syst., Signal Process.*, vol. 39, no. 2, pp. 919–960, Feb. 2020, doi: 10.1007/s00034-019-01248-1.
- [7] S. Mohan, J. Nandagopal, and S. Amritha, "Coupled dynamic control of unicycle robot using integral linear quadratic regulator and sliding mode controller," *Mater. Today, Process.*, vol. 5, no. 1, pp. 1447–1454, 2018.
- [8] S. Mohan, J. L. Nandagopal, and S. Amritha, "Decoupled dynamic control of unicycle robot using integral linear quadratic regulator and sliding mode controller," *Procedia Technol.*, vol. 25, pp. 84–91, 2016.
- [9] R. Wang, Q. Sun, X. Liu, and D. Ma, "Power flow calculation based on local controller impedance features for the AC microgrid with distributed generations," *IET Energy Syst. Integr.*, vol. 1, no. 3, pp. 202–209, Sep. 2019.
- [10] R. Wang, Q. Sun, D. Ma, and Z. Liu, "The small-signal stability analysis of the droop-controlled converter in electromagnetic timescale," *IEEE Trans. Sustain. Energy*, vol. 10, no. 3, pp. 1459–1469, Jul. 2019.
- [11] R. Wang, Q. Sun, Y. Gui, and D. Ma, "Exponential-function-based droop control for islanded microgrids," *J. Mod. Power. Syst. Clean Energy*, vol. 7, no. 4, pp. 899–912, 2019.
- [12] M. F. Hamza, H. J. Yap, I. A. Choudhury, H. Chiroma, and T. Kumbasar, "A survey on advancement of hybrid type 2 fuzzy sliding mode control," *Neural Comput. Appl.*, vol. 30, no. 2, pp. 331–353, Jul. 2018.
- [13] W. Ji, J. Qiu, and H. R. Karimi, "Fuzzy-model-based output feedback sliding mode control for discrete-time uncertain nonlinear systems," *IEEE Trans. Fuzzy Syst.*, early access, May 15, 2019, doi: 10.1109/TFUZZ.2019.2917127.
- [14] W. Ji, J. Qiu, L. Wu, and H.-K. Lam, "Fuzzy-affine-model-based output feedback dynamic sliding mode controller design of nonlinear systems," *IEEE Trans. Syst., Man, Cybern. Syst.*, early access, Mar. 12, 2019, doi: 10.1109/TSMC.2019.2900050.
- [15] K. Yin, K. Xiang, M. Pang, J. Chen, P. Anderson, and L. Yang, "Personalised control of robotic ankle exoskeleton through experience-based adaptive fuzzy inference," *IEEE Access*, vol. 7, pp. 72221–72233, 2019.
- [16] C. Aguilar-Ibáñez, J. H. Sossa-Azuela, and M. S. Suarez-Castanon, "A backstepping-based procedure with saturation functions to control the PVTOL system," *Nonlinear Dyn.*, vol. 83, no. 3, pp. 1247–1257, Feb. 2016.
- [17] P. Sindareh Esfahani and J. K. Pieper, "Robust model predictive control for switched linear systems," *ISA Trans.*, vol. 89, pp. 1–11, Jun. 2019.
- [18] M. M. Ferdaus, M. Pratama, S. G. Anavatti, M. A. Garratt, and E. Lughofer, "PAC: A novel self-adaptive neuro-fuzzy controller for micro aerial vehicles," *Inf. Sci.*, vol. 512, pp. 481–505, Feb. 2020.
- [19] J. de J. Rubio, L. Zhang, E. Lughofer, P. Cruz, A. Alsaedi, and T. Hayat, "Modeling and control with neural networks for a magnetic levitation system," *Neurocomputing*, vol. 227, pp. 113–121, Mar. 2017.
- [20] C.-F. Chen, Z.-J. Du, L. He, J.-Q. Wang, D.-M. Wu, and W. Dong, "Active disturbance rejection with fast terminal sliding mode control for a lower limb exoskeleton in swing phase," *IEEE Access*, vol. 7, pp. 72343–72357, 2019.
- [21] J. O. Escobedo-Alva, E. C. Garcia-Estrada, L. A. Paramo-Carranza, J. A. Meda-Campana, and R. Tapia-Herrera, "Theoretical application of a hybrid observer on altitude tracking of quadrotor losing GPS signal," *IEEE Access*, vol. 6, pp. 76900–76908, 2018.
- [22] J. A. Meda-Campana, "On the estimation and control of nonlinear systems with parametric uncertainties and noisy outputs," *IEEE Access*, vol. 6, pp. 31968–31973, 2018.
- [23] X. Yang, P. Wei, Y. Zhang, X. Liu, and L. Yang, "Disturbance observer based on biologically inspired integral sliding mode control for trajectory tracking of mobile robots," *IEEE Access*, vol. 7, pp. 48382–48391, 2019.
- [24] C. Aguilar-Ibanez, H. Sira-Ramirez, M. S. Suarez-Castanon, and R. Garrido, "Robust trajectory-tracking control of a PVTOL under crosswind," *Asian J. Control*, vol. 21, no. 3, pp. 1293–1306, May 2019.
- [25] C. Aguilar-Ibanez and M. S. Suarez-Castanon, "A trajectory planning based controller to regulate an uncertain 3D overhead crane system," *Int. J. Appl. Math. Comput. Sci.*, vol. 29, no. 4, pp. 693–702, Dec. 2019.
- [26] G. Puriel Gil, W. Yu, and H. Sossa, "Reinforcement learning compensation based PD control for a double inverted pendulum," *IEEE Latin Amer. Trans.*, vol. 17, no. 02, pp. 323–329, Feb. 2019.
- [27] M. Ramirez-Neria, G. Ochoa-Ortega, A. Luviano-Juarez, N. Lozada-Castillo, M. A. Trujano-Cabrera, and J. P. Campos-Lopez, "Proportional retarded control of robot manipulators," *IEEE Access*, vol. 7, pp. 13989–13998, 2019.
- [28] A. Mallem, N. Slimane, W. Benaziza, "Robust control of mobile robot in presence of disturbances using neural network and global fast sliding mode," *J. Intell. Fuzzy Syst.*, vol. 34, pp. 4345–4354, 2018.
- [29] J. Samiuddin, B. Badkoubeh, M. Sadeghassadi, J. K. Pieper, and C. J. B. Macnab, "A new robust weight update for cerebellar model articulation controller adaptive control with application to transcritical organic rankine cycles," *Trans. Inst. Meas. Control*, vol. 41, no. 10, pp. 2738–2750, Jun. 2019.
- [30] J. Sun, Y. Wang, Y. Yu, and C. Sun, "Nonlinear robust compensation method for trajectory tracking control of quadrotors," *IEEE Access*, vol. 7, pp. 26766–26776, 2019.
- [31] C. Zhao, C. Yu, and J. Yao, "Dynamic decoupling based robust synchronous control for a hydraulic parallel manipulator," *IEEE Access*, vol. 7, pp. 30548–30562, 2019.

- [32] R. Wang, Q. Sun, P. Zhang, Y. Gui, D. Qin, and P. Wang, "Reduced-order transfer function model of the droop-controlled inverter via Jordan continued-fraction expansion," *IEEE Trans. Energy Convers.*, early access, Mar. 12, 2020, doi: [10.1109/TEC.2020.2980033](https://doi.org/10.1109/TEC.2020.2980033).
- [33] W. Rui, S. Qiuye, M. Dazhong, and H. Xuguang, "Line impedance cooperative stability region identification method for grid-tied inverters under weak grids," *IEEE Trans. Smart Grid*, early access, Jan. 29, 2020, doi: [10.1109/TSG.2020.2970174](https://doi.org/10.1109/TSG.2020.2970174).
- [34] R. Wang, Q. Sun, D. Ma, and X. Zhang, "The equivalent impedance characteristic analysis of the AC microgrid and its decoupled power flow calculation," *Int. Trans. Electr. Energy Syst.*, vol. 29, no. 7, Jul. 2019, Art. no. e2820.



VICTOR GARCIA is currently pursuing the Ph.D. degree with the Sección de Estudios de Posgrado e Investigación, ESIME Azcapotzalco, Instituto Politécnico Nacional. He has published three articles in international journals. His fields of interest are robotic systems, modeling, and intelligent systems.



DANY IVAN MARTINEZ is currently pursuing the Ph.D. degree with the Sección de Estudios de Posgrado e Investigación, ESIME Azcapotzalco, Instituto Politécnico Nacional. He has published four articles in international journals. His fields of interest are robotic systems, modeling, and intelligent systems.



GENARO OCHOA received the Ph.D. degree from the Sección de Estudios de Posgrado e Investigación, ESIME Azcapotzalco, Instituto Politécnico Nacional, in 2017. He has published ten articles in international journals. His fields of interest are robotic systems, modeling, and intelligent systems.



JOSÉ DE JESÚS RUBIO (Member, IEEE) is currently a full-time Professor with the Sección de Estudios de Posgrado e Investigación, ESIME Azcapotzalco, Instituto Politécnico Nacional. He has published more than 139 international journal articles with 2089 cites from Scopus. He serves on the Editorial Board for the IEEE TRANSACTIONS ON NEURAL NETWORKS AND LEARNING SYSTEMS, the IEEE TRANSACTIONS ON FUZZY SYSTEMS, *Neural Computing and Applications*, *Frontiers in Neuro-*

robotics, the *Journal of Intelligent and Fuzzy Systems*, *Mathematical Problems in Engineering*, *International Journal of Advanced Robotic Systems*, the IEEE LATIN AMERICA TRANSACTIONS, *Evolving Systems*, and the *International Journal of Business Intelligence and Data Mining*. He is a Guest Editor of *Neurocomputing*, *Applied Soft Computing*, *Sensors*, the *Journal of Real-Time Image Processing*, the *Journal of Supercomputing*, the *International Journal of Applied Mathematics and Computer Science*, and *Computational Intelligence and Neuroscience*. He has been the tutor of four Ph.D. degree students, 19 Ph.D. degree students, 42 M.S. degree students, four S. degree students, and 17 B.S. degree students.



RICARDO BALCAZAR received the Ph.D. degree from the Sección de Estudios de Posgrado e Investigación, ESIME Azcapotzalco, Instituto Politécnico Nacional, in 2017. He has published nine articles in international journals. His fields of interest are robotic systems, modeling, and intelligent systems.



DAVID RICARDO CRUZ received the Ph.D. degree from the Sección de Estudios de Posgrado e Investigación, ESIME Azcapotzalco, Instituto Politécnico Nacional, in 2018. He has published eight articles in international journals. His fields of interest are robotic systems, modeling, and intelligent systems.



TOMAS MIGUEL VARGAS is currently pursuing the Ph.D. degree with the Sección de Estudios de Posgrado e Investigación, ESIME Azcapotzalco, Instituto Politécnico Nacional. He has published three articles in international journals. His fields of interest are robotic systems, modeling, and intelligent systems.



ARTURO AGUILAR received the Ph.D. degree from the Sección de Estudios de Posgrado e Investigación, ESIME Zacatenco, Instituto Politécnico Nacional, in 2020. He has published seven articles in international journals. His fields of interest are robotic systems, modeling, and intelligent systems.



JUAN FRANCISCO NOVOA received the Ph.D. degree from the Sección de Estudios de Posgrado e Investigación, ESIME Zacatenco, Instituto Politécnico Nacional, in 2020. He has published eight articles in international journals. His fields of interest are robotic systems, modeling, and intelligent systems.



CARLOS AGUILAR-IBAÑEZ is currently a full-time Professor with the Centro de Investigación en Computación, Instituto Politécnico Nacional. He has published 80 articles in international journals. His fields of interest are robotic systems, modeling, and intelligent systems.

...